Desalination and Water Treatment
www.deswater.com

doi:10.5004/dwt.2022.28310

253 (2022) 256–269
March

Adsorption properties of lead and zinc ions onto iminodiacetic acid functionalized loofah from solution

Junli Wang[a], Xu Liu[a,*], Huayun Han[b], Runping Han[a,*]

[a]*College of Chemistry, Green Catalysis Center, Zhengzhou University, No 100 of Kexue Road, Zhengzhou, 450001 China, emails: lxcod@zzu.edu.cn (X. Liu), rphan67@zzu.edu.cn (R. Han), 953403789@qq.com (J. Wang)*
[b]*Center for Modern Analysis and Gene Sequencing, Zhengzhou University, No 100 of Kexue Road, Zhengzhou, 450001 China, email: ryan@zzu.edu.cn*

Received 1 September 2021; Accepted 14 February 2022

ABSTRACT

Lead and zinc ions in water are very unfriendly to humans and the environment. In this experiment, an environmental friendly and hydroxyl-rich biomass materials loofah (LG) was modified by epichlorohydrin and iminodiacetic acid (IDA). IDA-LG was used to remove Pb^{2+} and Zn^{2+} as model pollutants. X-ray photoelectron spectroscopy, scanning electron microscopy, etc were used for characterizing the prepared adsorbent. The results suggested that the adsorbent had a non-mesoporous structure while IDA modification was successful. The effects of pH, salinity, temperature and time on adsorption were investigated through batch adsorption experiments. High acidity and salinity have negative effects on adsorption. The theoretical adsorption capacity of IDA-LG for Pb^{2+} and Zn^{2+} could reach 82.5 and 25.2 mg g^{-1} at 303 K, respectively. Mechanism of adsorption was coordination and ion exchange. In the binary system, there was higher affinity about IDA-LG for Pb^{2+}. There was good regenerative property of spent IDA-LG. IDA-LG could be used as a novel adsorbent to remove heavy metals from the sewage.

Keywords: Adsorption; Lead ion; Zinc ion; Modified loofah; Regeneration

1. Introduction

Water plays an important role in the process of life. With the economic flourishing growth and population explosion, industrialization process has been accelerated, and the development of mining operations, fertilizer industry and battery electroplating, many mixtures containing various pollutants has been discharged into the environment without treatment, resulting in serious water pollution. Among several common pollution types, Heavy metals have become one of the more serious existing pollutions [1]. Heavy metals are non-degradable, so they are easy to accumulate in the environment. Heavy metal ions with high content and toxicity in water environment include mercury, arsenic, copper, lead, zinc and so on [2]. These heavy metals lead serious impact to human health and other organisms. Pb(II) is serious toxic metals in nature. According to WHO regulations, the maximum allowable concentration in the environment is 0.01 mg L^{-1}. Even at a trace level, Pb(II) can accumulate in organisms and leads serious damage to the blood, kidney and nervous system, and even leads to cancer, especially the damage to children's health and intelligence [3–6]. Similarly, Zinc is also heavy metals in water and environment. Although it is an essential trace element in body, it involved in regulating many physiological functions and many biochemical processes. However, excessive zinc can lead to poisoning and cause prominent health problems, such as cell damage, ischemia, etc. [2,7]. Therefore, it is significantly important to remove Pb and Zn ions to purify water.

* Corresponding authors.

At present, the methods of treatment with heavy metal or organic wastewater contain chemical precipitation, ion exchange, adsorption, membrane filtration, and some biotechnology [8–10]. Among them, adsorption method is widely used to remove pollutants in water because of its simple operation and high efficiency. Common adsorbents include activated carbon, graphene oxide, zeolite, nanocomposites, biomass materials and so on [11,12]. Compared with other materials, biomass materials have wide sources, low price, renewable and less environmental pollution. Therefore, it is widely used as a new adsorbent [13,14]. Biomass commonly used in adsorption materials is wheat straw [15], bagasse [16], corn cob, walnut shell [17], sawdust, peanut shell [18]. These biomass materials are rich in cellulose and hemicellulose, so they have been studied by more and more researchers. Tian et al. [19] synthesized magnetic wheat straw by co-precipitation and used it to remove As(III) from wastewater, which represented good characteristics at pH = 3. Elizalde-González et al. [20] modified corncobs with quaternary amine, and the removal efficiency of methyl orange was 68%.

As a natural plant fiber, loofah has cellulose (60%) and hemicellulose (30%) as high as 90%. Because of its unique three-dimensional porous fiber structure, water immersion resistance, acid and alkali resistance, high mechanical strength and flexibility, it has become a potential adsorption material [21]. Luffa can not only be directly used as an adsorption material, but also be used as a matrix, carrying functional groups to improve the adsorption effect [22]. Pathania et al. [23] prepared methyl acrylate and acrylic acid modified loofah by microwave irradiation using grafting agent, and the functionalized loofah with the highest grafting ratio was obtained. Theoretical adsorption quantity of adsorption material for Congo red dye was 19.24 mg g^{-1}. Iminodiacetic acid (IDA) is a good chelating agent with two carboxyl groups and a tertiary nitrogen atom. This property of IDA makes it to have high affinity to bind heavy metals with positive charge via the formation of a coordination covalent bond. Based on this characteristic, many researchers regard IDA as a modified material, which is used to modify materials, thus improving the properties of materials [10]. The magnetic peanut shell was modified with IDA by Aryee et al. [24], and the new material (PN-Fe_3O_4-IDA) was used to remove Pb and Cu in water. The maximum absorption capacity was 0.36 and 0.75 mmol g^{-1}, respectively, which showed that the adsorbent modified by IDA showed remarkable adsorption ability and some unique characteristics for selected pollutants. Zhang [25] prepared a series of carboxylic functionalized materials (X-IDA-EPI-OCS) based on natural corn stalks by modifying corn stalks with iminodiacetic acid. The adsorption capacity of X-IDA-EPI-OCS to Ga(III) in acidic solution could arrived at 139.56 mg g^{-1}. The above research shows that the materials modified by IDA show excellent adsorption characteristics.

Naushad et al. [26] synthesized starch-based ZnO nanocomposites (CST-ZnO) for efficient removal of Pb(II) ions from water. The maximum Langmuir adsorption capacity of CST-ZnO nanocomposites is 256.4 mg g^{-1}. Wang et al. [27] synthesized GO by modified Hummers method. The maximum adsorption capacity for Zn(II) was 246 mg g^{-1} at 20°C. However, compared with this study, the reagents used in the above studies are not green and simple because they are expensive and complicated in synthesis and are not conducive to solid–liquid separation.

The aim of this study is to prepare IDA modified loofah by crosslinking iminodiacetic acid with epichlorohydrin, and the new material (IDA-LG) was used to remove Pb^{2+} and Zn^{2+} from aqueous solution. The experimental indicated the adsorption capacity of loofah was improved after modification with good selectivity for Pb. It is proved that the modification method is effective, and the prepared materials are green and novel. So this study is of significance.

2. Experiments and methods

2.1. Materials and reagents

The main reagents are ethanol, epichlorohydrin, sodium hydroxide, anhydrous sodium carbonate, iminodiacetic acid, lead nitrate hexahydrate, zinc sulfate heptahydrate, calcium nitrate, sodium nitrate, hydrochloric acid, nitric acid, etc. The lead nitrate and zinc sulfate solutions with different concentrations used in the experiment were all diluted from the stock solution.

2.2. Preparation of IDA-LG

The raw material was treated with 5% sodium hydroxide solution in 60°C water bath for 6 h. The processed loofah was washed with distilled water and dried, and then processed into filaments with a pulverizer. Then, the alkali-treated loofah was epoxidized and amino-acetated. According to the reported literature [28]: added 4.0 g loofah sponge into 500 mL conical flask, then added 200 mL 3 mol L^{-1} sodium hydroxide, 60 mL epichlorohydrin and 40 mL absolute ethyl alcohol, put the conical flask in a constant temperature oscillator at 50°C and shake it for 3 h. Next, it was washed with ethyl alcohol and dried after the reaction. Then placed the epoxidized product in a 500 mL conical flask, added 120 mL 1.0 mol L^{-1} sodium carbonate solution and 4.0 g iminodiacetic acid, adjusted the pH to 11 with 3 mol L^{-1} sodium hydroxide. Stirred at 65°C for 6 h, obtained the loofah modified by iminodiacetic acid (IDA-LG). Fig. 1 shows the preparation process of IDA-LG in detail, and Fig. 2 shows the reaction mechanism diagram.

2.3. Characterization

The morphology and surface chemistry of the material can be characterized by the following ways. The isoelectric point characterizes the positive and negative charges on the surface of material. So, the isoelectric points of LG and IDA-LG were measured by solid-phase additive process. Measuring specific surface area and pore volume according to Brunauer–Emmett–Teller (BET) surface area; X-ray photoelectron spectroscopy was used to measure the element composition and adsorption process before and after adsorption. The microstructure and morphology of the material were imaged by scanning electron microscopy. The characteristic functional groups of LG and IDA-LG were determined by Fourier-transform infrared spectroscopy in the range of 400–4,000 wave numbers (cm^{-1}).

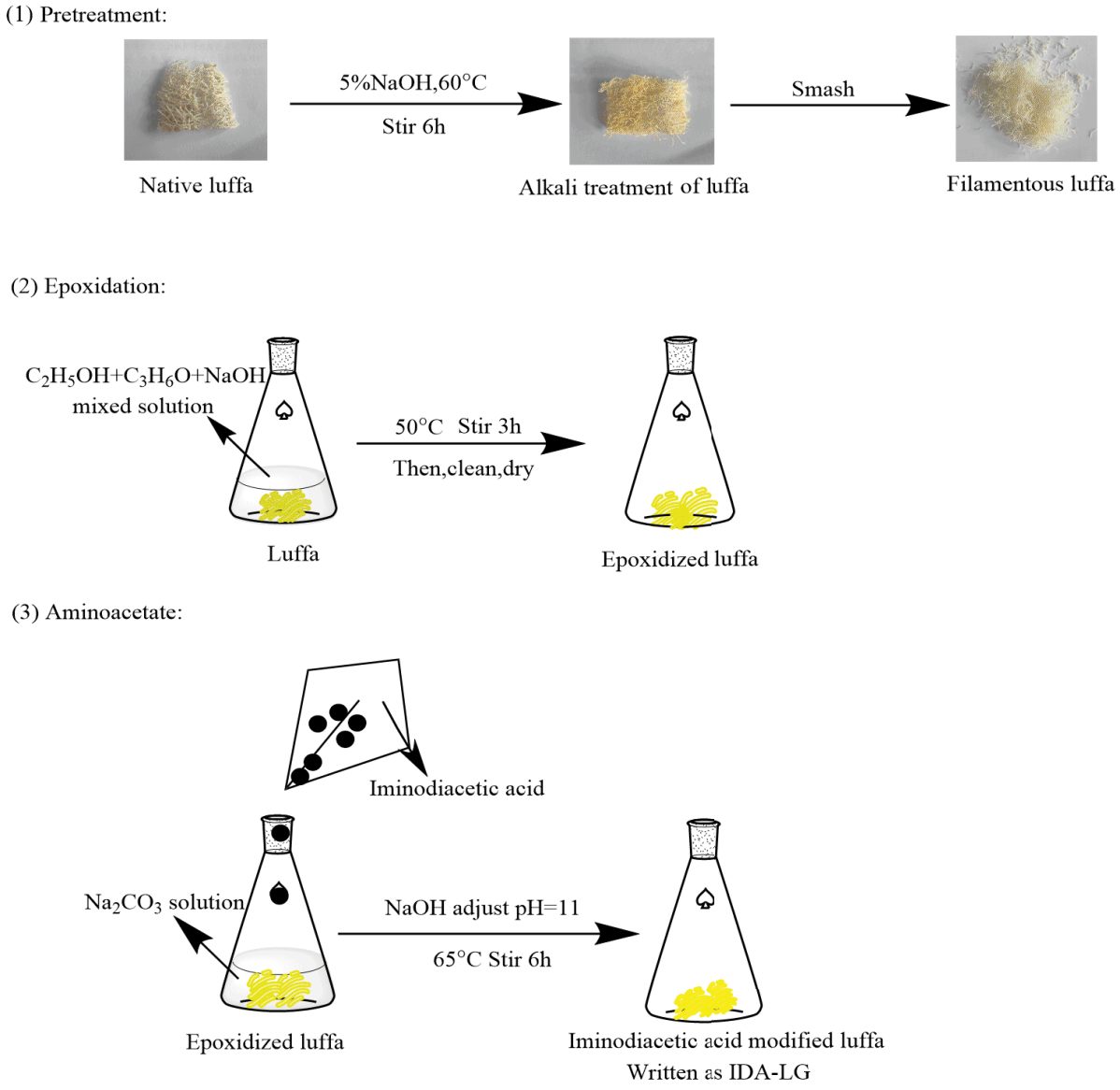

Fig. 1. The preparation process of IDA-LG (1) pretreatment, (2) epoxidation, (3) aminoacetate.

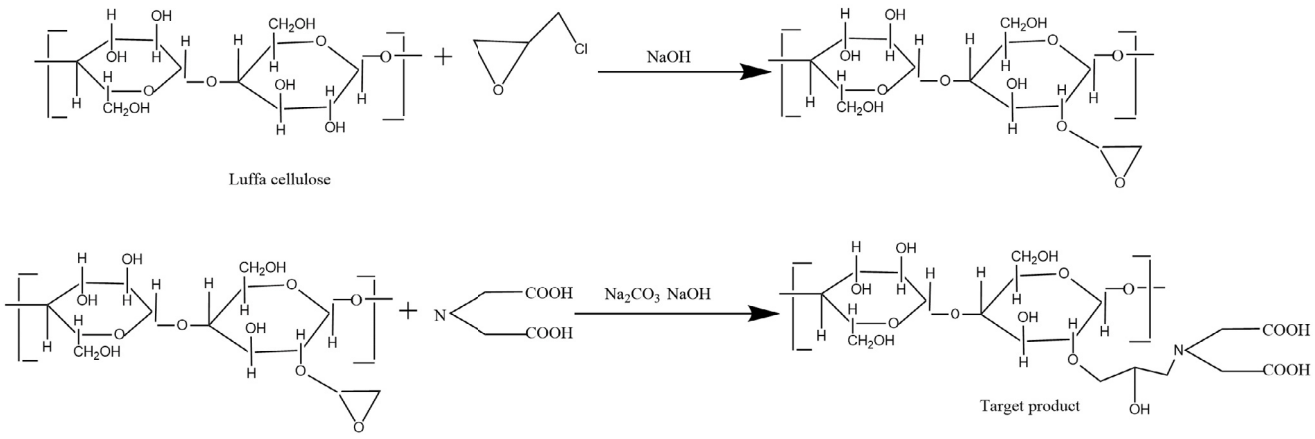

Fig. 2. The synthetic mechanism of IDA-LG.

2.4. Batch adsorption experiment

The experiment mainly studies the adsorption properties of adsorbent toward Pb^{2+} or Zn^{2+}. The influence of pH, salinity, temperature and time on Pb^{2+} and Zn^{2+} is performed [29]. A number of 50 mL conical flask were taken and 0.010 g adsorbent was added into the adsorbate solution with the concentration of C_0 (mg L^{-1}), V = 10.0 mL. Sealed and oscillated in a thermostatic oscillator. After filtration, the concentration C_t (mg L^{-1}) of the remaining adsorbate was measured with a flame atomic absorption spectrometer. The unit adsorption capacity q_e (mg g^{-1}) of adsorbent is calculated by Eq. (1).

$$q = \frac{V\left(C_0 - C\right)}{m} \tag{1}$$

where m is the mass (g) of adsorbent, V is the volume (L) of adsorbate solution, C_0 and C are the concentration of Pb^{2+} or Zn^{2+} before and after adsorption (mg L^{-1}).

2.5. Desorption regeneration

In order to explore whether adsorption materials can be recycled and maximize the value of adsorption materials, the spent materials are desorbed and regenerated using acid, alkali, salt and ethanol. Firstly, the adsorbate solution with a certain concentration was selected to achieve adsorption saturation, and the unit adsorption capacity (q_e) was measured and calculated at this time. Rinsing the adsorbent to neutral with distilled water, and then selected different desorption solutions to re-adsorb the adsorbent, and calculated the unit adsorption capacity of the regenerated adsorbent as q_r. Selected the desorption solution with the best desorption regeneration effect to desorb and regenerate the adsorbent several times. The desorption rate (d) and regeneration rate are calculated by Eqs. (2) and (3).

$$d = \frac{m_d}{m_0} \times 100\% \tag{2}$$

$$r = \frac{q_r}{q_e} \times 100\% \tag{3}$$

where m_d is the mass (mg) of adsorbate desorbed during desorption, and m_0 is the mass (mg) of adsorbent on adsorbent before desorption.

2.6. Error analysis

The curve obtained from the experiment was fitted nonlinearly, and the sum of squares of errors (SSE) was obtained. SSE as one of the basis can judge whether the model is in conformity with the requirement. It has practical application value and its formula is as follows:

$$\mathrm{SSE} = \sum\left(q - q_c\right)^2 \tag{4}$$

where q_c and q are the theoretical adsorption capacity and experimental adsorption capacity, respectively.

3. Results and discussion

3.1. Characterization of LG and IDA-LG

3.1.1. Solution pH of the point of zero charge

Using PHS-3C instrument to measure the zero charge point pH value (pH_{pzc}) of LG and IDA-LG and the results are shown in Fig. 3. The isoelectric point of LG was 6.54. After IDA grafting, the isoelectric point of IDA-LG changed to 5.06 (pK_a value of IDA was 3.81) [30]. After modification, the isoelectric point moved to acidic direction, which was because the carboxyl and tertiary nitrogen structure of iminodiacetic acid made the isoelectric point of adsorption material smaller, which proved that iminodiacetic acid was successfully grafted onto loofah.

3.1.2. BET of materials

The specific surface area of original loofah was 0.0285 m^2 g^{-1}, which was 0 after modification. The reason may be that LG was treated with NaOH, the lignin on the surface was destroyed, which leaded to the reduction of the pore volume of IDA-LG, and the internal microporous structure was blocked after IDA grafting [31]. On the other hand, it is proved that the adsorbent mainly relies on the surface functional group for adsorption.

3.1.3. Fourier-transform infrared spectroscopy analysis

Fourier-transform infrared spectroscopy (FTIR) could provide information on the surface functional groups of materials. Fig. 3 is the FTIR diagram of LG and IDA-LG. It was clearly shown that there was a wide strong absorption peak at 3,300–3,500 cm^{-1} before modification, which was the stretching vibration absorption peak of intramolecular –OH, mainly from cellulose, hemicellulose and polysaccharide [32,33]. After modification, the peak of the material got widened at 3,000~3,500 cm^{-1}, it was because of the expansion and contraction vibration of –N–H and the introduction of more carboxyl groups. Absorption peak at 1,720 cm^{-1} was the stretching vibration of –C=O, which was from hemicellulose or lignin and carboxylic acid. After modification, the peak at 1,270 cm^{-1} became strong and sharp, which proved that the number of carboxyl groups in the modified material increases. The frame vibration of benzene ring was at 1,606, 1,495, 1,466 cm^{-1}. After modification, the skeleton vibration peak of benzene ring disappeared because NaOH destroyed the structure of lignin. The peak of the modified material at 1,072 cm^{-1} became wide. It was the stretching vibration peak of –C–N [34]. Those above analysis showed that iminodiacetic acid was successfully grafted onto loofah.

3.1.4. Scanning electron microscopy of materials

Fig. 4 shows the scanning electron microscopy (SEM) of LG and IDA-LG. It could be seen that the original loofah was smooth and the structure was arranged neatly [35]. There were micropores, because its surface contains lignin, cellulose and some inorganic salts. In Fig. 4b, the surface of the modified adsorbent was uneven and micropores disappear.

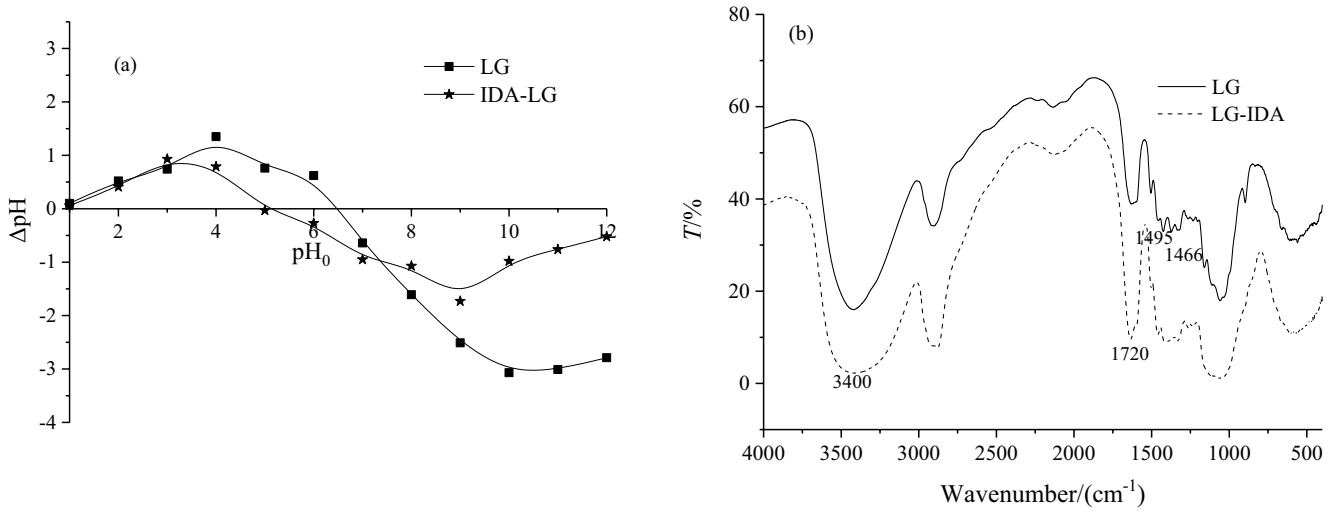

Fig. 3. Isoelectric point (a) and FTIR (b) of the LG and IDA-LG.

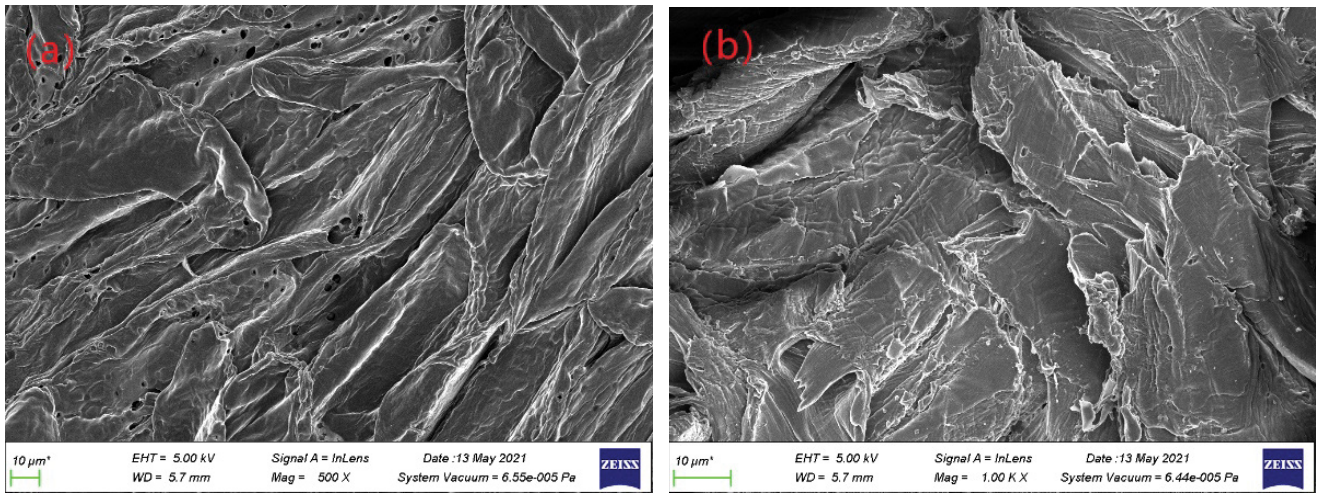

Fig. 4. Scanning electron microscopy of (a) LG and (b) IDA-LG.

This may be because the lignin and other structures on the surface are destroyed after NaOH treatment, and the inner cellulose was exposed, so that iminodiacetic acid was easier to graft. The disappearance of micropores was consistent with the change of materials from micro-mesopores to non-mesopores in BET characterization, so it could be inferred from two SEM imaged that iminodiacetic acid was successfully grafted onto loofah sponge.

3.2. Batch adsorption study

3.2.1. Effect of solution pH

The pH value, which affects the electrostatic force, is an important parameter in the adsorption process, thus affects the adsorption of metal ions onto adsorbent. Fig. 5 presents the unit adsorption capacity of Pb^{2+} and Zn^{2+} increased with the increase of pH (the pH range of Pb^{2+} solution was from 1 to 5.20, initial solution pH 5.20 without adjustment). The pH range of Zn^{2+} solution was from 1 to 5.42 (initial solution pH 5.42). Values of q_e about IDA-LG increased from 67.1 to 82.7 mg g^{-1} for Pb^{2+} and 17.3 to 22.6 mg g^{-1} for Zn^{2+}. The main reason was that with the increase of solution acidity, the free H^+ increased, competing with Pb^{2+} and Zn^{2+} for adsorption sites, resulting in the decrease of unit adsorption capacity. Combined with isoelectric point analysis, the isoelectric point of IDA-LG was 5.06, when pH < 5.06, the surface of IDA-LG presented positive charge, which had electrostatic repulsion with Pb^{2+} and Zn^{2+}. When pH > 5.06, the surface of IDA-LG presented negative charge, which had electrostatic attraction with Pb^{2+} and Zn^{2+}. Therefore, it could be speculated that there may be electrostatic force during the adsorption process. It was also found that there was still some adsorption quantity at pH = 1. This showed that there was some resistance of acid for IDA-LG.

Keeping the solution temperature at 303 K, C_0 = 180 mg L^{-1} for Pb^{2+} (pH 5.20), after reaching the adsorption equilibrium, the unit adsorption capacity of LG to Pb^{2+} was 29.7 mg g^{-1},

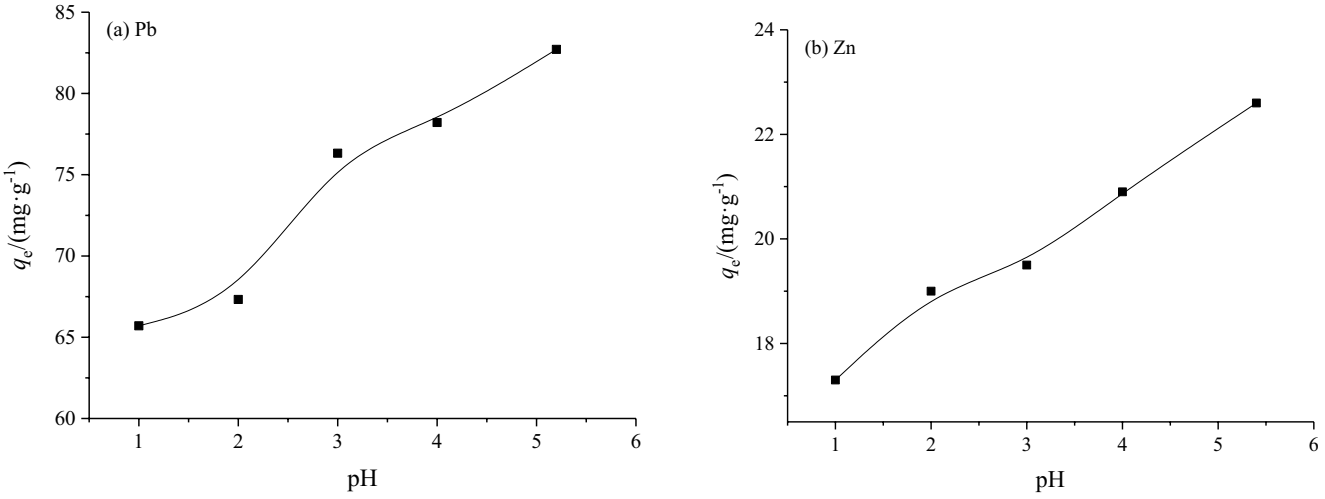

Fig. 5. Effect of pH on the adsorption of Pb^{2+} (a) and Zn^{2+} (b) by IDA-LG.

and that of IDA-LG to Pb^{2+} was 82.5 mg g^{-1}. Similarly, at C_0 = 50 mg L^{-1} for Zn^{2+} (pH 5.42), the unit adsorption capacity of LG and IDA-LG for Zn^{2+} were 3.8 and 25.2 mg g^{-1}. The adsorption performance of IDA-LG for Pb^{2+} and Zn^{2+} were better than that of LG. This proved that there were more functional groups on the material modified by iminodiacetic acid to provide adsorption sites, which is conducive to metal ion adsorption.

3.2.2. Effect of salinity

The actual heavy metal wastewater also contains a certain amount of Na^+, Ca^{2+} and Mg^{2+}, etc. The existence of these metal salt cations may affect the adsorption quantity of Pb^{2+} and Zn^{2+} on IDA-LG. So it is necessary to explore the effect of salinity on adsorption and the results are presented in Fig. 6. In Fig. 6a, with the increase of salinity, the unit adsorption capacity decreased slowly. In Fig. 6b, the effect of salinity on adsorption of Zn^{2+} was consistent with that of Pb^{2+}, and the influence of Ca^{2+} was greater than that of Na^+ in the two adsorption systems. Therefore, it could be considered that there existed competitive adsorption and electrostatic attraction between Pb^{2+} (Zn^{2+}) and IDA-LG. The same results were obtained in other studies, such as Fe_3O_4 and iminodiacetic acid modified peanut husk for binding Cu^{2+} and Pb^{2+} [26], carbon nanotubes as adsorbents for removal of Pb^{2+} [36] and leonardite as adsorbent for uptake Cd^{2+} and Zn^{2+} [37].

However, with the increase of salt concentration from 0 to 0.2 mol L^{-1}, the values of q_e is from 85.2 to 63.1 mg g^{-1} for Pb^{2+} and 22.1 to 15.0 mg g^{-1} for Zn^{2+}. This implied that there be still some adsorption quantity and other action (complexation) can be existed between metal ions and IDA-LG.

3.2.3. Study on the influence of metal ion concentration and adsorption isotherm

Adsorption isotherm curves are presented in Fig. 7. With the increase of the concentration of Pb^{2+}, it could be known from Fig. 7a that the unit adsorption capacity increased, this was because the concentration gradient on the surface of IDA-LG increased, more Pb^{2+} was bound to the surface of the adsorbent, and finally reached the adsorption platform. Analyzed from the aspect of temperature, when the temperature gradually rose, the unit adsorption capacity of the same concentration also increased. It proved that the adsorption of Pb^{2+} on IDA-LG was an endothermic process. When the initial concentration of Pb^{2+} was 180 mg L^{-1}, the unit adsorption capacity was 64.1, 77.9, 86.3 mg g^{-1} at 293, 303 and 313 K, respectively. As shown in Fig. 7b, when the initial concentration of Zn^{2+} was 50 mg L^{-1}, values of q_e were 18.8, 20.7, 21.3 mg g^{-1} at three temperatures, respectively.

Adsorption isotherms represent the surface characteristics of adsorbents. In this paper, three isotherm models are used to fit the experimental data nonlinearly [38].

Expression of Langmuir model:

$$q_e = \frac{q_m K_L C_e}{1 + K_L C_e} \tag{5}$$

where q_m denotes the maximum adsorption capacity (mg g^{-1}); C_e reflects the equilibrium concentration (mg L^{-1}); K_L means Langmuir adsorption equilibrium constant (L mg^{-1}). This model is used to describe whether the reaction is homogeneous adsorption.

Expression of Freundlich model:

$$q_e = K_L C_e^{1/n} \tag{6}$$

where $1/n$ means adsorption strength of adsorbent and it is related to the degree of unevenness. The closer $1/n$ is to 0, the more uneven the surface of the adsorbent. $0.1 < 1/n < 1$, the adsorption was easy, $1/n \geq 2$, the adsorption was difficult. K_F notes one parameter of this model.

Expression of Koble–Corrigan model:

$$q_e = \frac{AC_e^n}{1 + BC_e^n} \tag{7}$$

where A, B and n represent all model constants. This model is a three-parameter equation. It is a combination of Freundlich and Langmuir models. When n is close to 1, it means that this model is closer to the Langmuir, and when $0 < n < 1$, it is close to Freundlich model.

Three models are used to fit the isotherm data of IDA-LG adsorption of Pb^{2+} and Zn^{2+}, and the fitting results are shown in Fig. 7 and Table 1. For Pb^{2+}, values of R^2 from Koble–Corrigan model was over 0.93 and SSE value was small (Table 1), which could be used to describe adsorption behavior. Moreover, the fitting curves from Koble–Corrigan model were also very close to the experimental curves. Parameter n from Koble–Corrigan model approached to one, this is more inclined to Langmuir model. In the Langmuir model, the values of $q_{e(exp)}$ and q_m were not significantly different, and values of R^2 were larger than that of Freundlich model, the data analysis was in keeping with the Koble–Corrigan model. Therefore, the reaction was dominated by monolayer adsorption.

For Zn^{2+}, values of R^2 of Koble–Corrigan and Freundlich model were both larger than 0.9, and SSE values were smaller, so both models could describe the adsorption process. In Koble–Corrigan model, n value was between 0 and 1, and the model was more inclined to Freundlich model. The fitting curves from Freundlich model were close to the experimental curves. In Freundlich model, as there was $0.1 < 1/n < 1$, IDA-LG was easy to adsorb Zn^{2+} under experimental conditions, which indicated that the adsorption process of IDA-LG to Zn^{2+} was heterogeneous adsorption.

3.2.4. Study on the influence of time and adsorption kinetics

It is important to study the effect of contact time on adsorption quantity and the results at 293, 303 and 313 K are presented in Fig. 8. The adsorption of Pb^{2+} and Zn^{2+} onto IDA-LG could be divided into three stages: rapid adsorption, medium-speed adsorption and slow-speed adsorption.

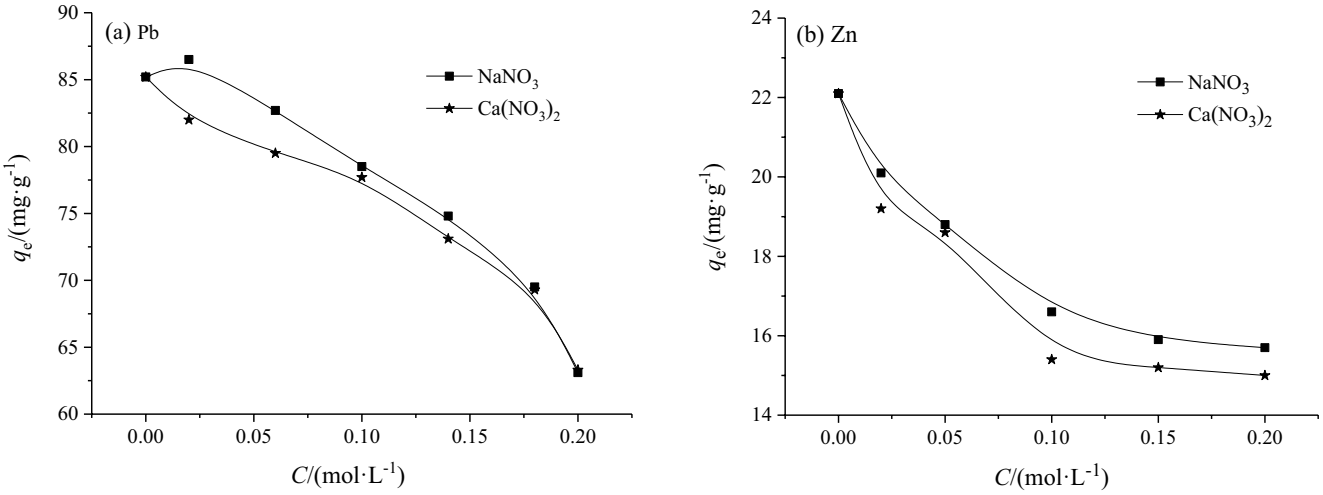

Fig. 6. Effect of salinity on the adsorption of Pb^{2+} (a) and Zn^{2+} (b) by IDA-LG.

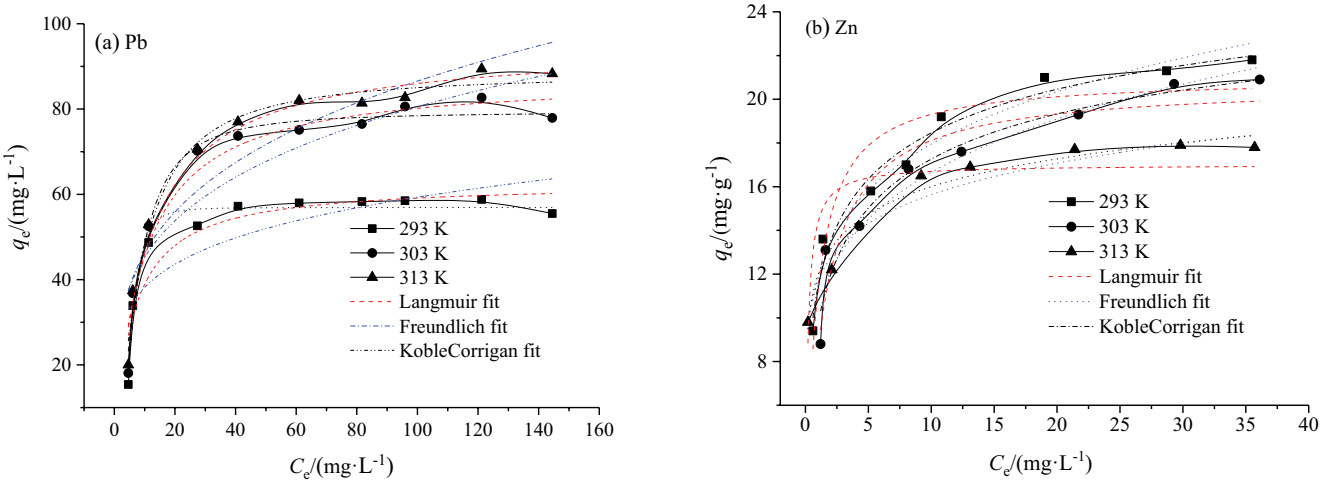

Fig. 7. Effect of Pb^{2+} (a) and Zn^{2+} (b) concentration on adsorption and fitted isotherm curves.

Table 1
Results of isotherm model fitting of Pb^{2+} and Zn^{2+} adsorption by IDA-LG

			Langmuir			
	T (K)	K_L (L mg^{-1})	$q_{e(exp)}$ (mg g^{-1})	q_m (mg g^{-1})	R^2	SSE × 10^2
Pb^{2+}	293	0.155 ± 0.041	58.8	62.7 ± 3.0	0.855	0.295
	303	0.108 ± 0.018	86.7	87.6 ± 3.1	0.947	0.248
	313	0.095 ± 0.012	89.4	95.1 ± 2.6	0.972	0.158
Zn^{2+}	293	5.42 ± 2.31	17.0	16.8 ± 1.2	0.611	0.036
	303	0.701 ± 0.145	20.7	20.7 ± 0.8	0.901	0.017
	313	1.15 ± 0.23	21.3	21.0 ± 0.8	0.884	0.022
			Freundlich			
	T (K)	K_F	1/n	R^2	SSE × 10^2	
Pb^{2+}	293	24.6 ± 5.5	0.191 ± 0.053	0.641	0.729	
	303	25.4 ± 5.4	0.250 ± 0.059	0.794	0.962	
	313	24.7 ± 4.6	0.272 ± 0.044	0.860	0.781	
Zn^{2+}	293	11.7 ± 0.5	0.127 ± 0.016	0.925	0.052	
	303	11.2 ± 0.7	0.197 ± 0.023	0.925	1.32	
	313	11.8 ± 0.6	0.181 ± 0.017	0.951	0.923	
			Koble–Corrigan			
	T (K)	A	B	n	R^2	SSE × 10^2
Pb^{2+}	293	0.189 ± 0.208	0.003 ± 0.004	3.24 ± 0.630	0.965	0.072
	303	2.37 ± 1.23	0.030 ± 0.015	1.72 ± 0.264	0.975	0.118
	313	4.70 ± 1.86	0.053 ± 0.020	1.34 ± 0.19	0.978	0.125
Zn^{2+}	293	18.1 ± 9.4	0.508 ± 0.760	0.207 ± 0.136	0.949	0.835
	303	15.1 ± 2.3	0.548 ± 0.243	0.487 ± 0.242	0.929	1.24
	313	18.2 ± 2.9	0.593 ± 0.253	0.404 ± 0.139	0.962	0.715

For Pb^{2+}, taking 293 K as an example, the rapid adsorption stage was 0–20 min, and the unit adsorption capacity increases rapidly with the increase of time; 20–60 min was the medium-speed adsorption stage, with the increase of time, the increase of unit adsorption capacity decreases significantly; 60~160 min was the slow adsorption stage, at this time the reaction tended to equilibrium. At three different initial concentrations (40, 80, 180 mg L^{-1}), with the increase of initial concentration, more adsorbate in the solution migrated to the surface of adsorbent, which directly resulted in the increase of adsorption quantity and the time required to reach equilibrium. With the increase of temperature, the equilibrium time became shorter, which proved that it was an endothermic reaction, and the experimental results were consistent with the influence of equilibrium concentration and temperature.

In the same way, the influence of time and initial concentration on the adsorption of Zn^{2+} by IDA-LG was consistent with the adsorption of Pb^{2+}. With the increase of time, the increase rate of unit adsorption capacity slows down and the overall trend was still rising. With the increase of concentration, the unit adsorption capacity increased when it arrived at equilibrium. With the increase of temperature, the equilibrium time decreased, the adsorption process was an endothermic process, which was consistent with the isotherm results.

Kinetics reflects the mechanism of adsorption reaction and the steps of reaction speed control, so it is very necessary to explore in practical research. To explore kinetic study in detail about IDA-LG toward Pb^{2+} and Zn^{2+}, pseudo-second-order kinetic equation and Elovich equation are selected to fit the data nonlinearly [39].

The expression of pseudo-second-order equation model is: the equation expression of the pseudo-second-order equation model is as follows:

$$q_t = \frac{k_2 q_e^2 t}{1 + k_2 q_e t} \tag{8}$$

where k_2 notes the rate constant (g mg^{-1} min^{-1}). This model can be used to describe the rate control step of adsorption reaction as chemical adsorption.

Expression of Elovich equation model is:

$$q_t = \frac{\ln(\alpha\beta)}{\beta} + \frac{\ln t}{\beta} \tag{9}$$

where α denotes the initial adsorption rate constant (g mg^{-1} min^{-1}) while β means the adsorption constant. Elovich equation model describes that the reaction mechanism is ion exchange.

The fitting results are presented in Table 2 and the fitted curves are also depicted in Fig. 8. It was drawn from the Table 2 that for the adsorption of Pb^{2+} and Zn^{2+} onto IDA-LG, the R^2 values of pseudo-second-order equation were larger ($R^2 > 0.90$), and SSE values were smaller for both metal ions. The theoretical equilibrium adsorption capacity was close to the experimental value. Furthermore, the fitted curves (Fig. 8) of Pb^{2+} and Zn^{2+} from pseudo-second-order equation were closer to experimental results at one condition. So this model could describe the adsorption kinetic behavior. There was chemical role between adsorbates and adsorbent. For Elovich equation, there were also higher values of R^2 and smaller values of SSE. Therefore, this model was also suitable to predict the kinetic process and ion exchange was participated in the adsorption process. In summary, the adsorption behavior of IDA-LG for Pb^{2+} and Zn^{2+} mainly was chemisorption, accompanied by ion exchange.

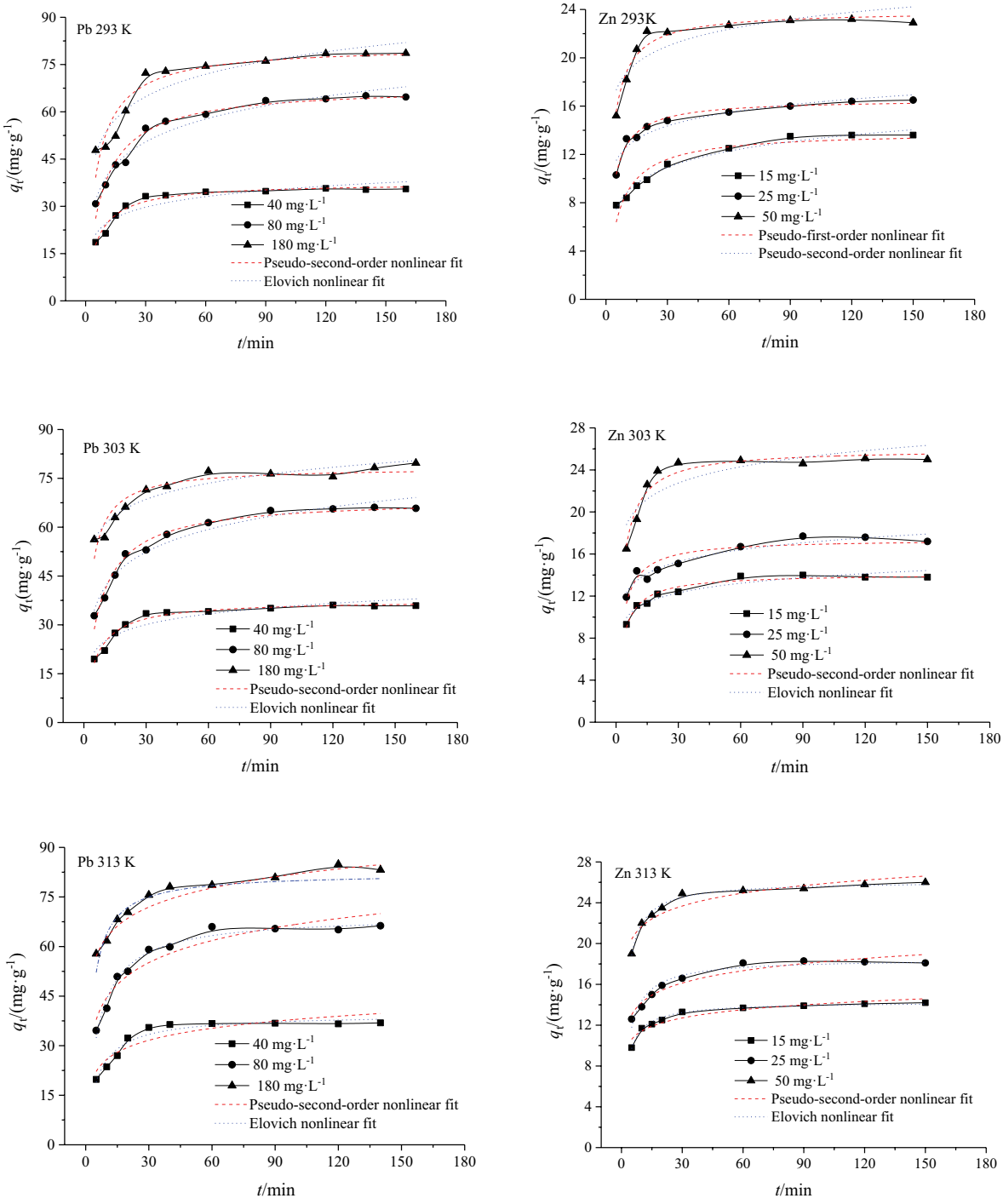

Fig. 8. Effects of contact time and fitted kinetic curves at various temperatures about Pb^{2+} (left) and Zn^{2+} (right).

Table 2
Kinetic nonlinear fitting results of adsorption of Pb^{2+} and Zn^{2+} by IDA-LG

	Pseudo-second-order equation						
	T (K)	C_0 (mg L^{-1})	$q_{e(exp)}$ (mg g^{-1})	$q_{e(theo)}$ (mg g^{-1})	k_2 (g mg^{-1} min^{-1})	R^2	SSE × 10^2
	293	40.0	35.7	37.4 ± 0.6	0.005 ± 5.49	0.960	1.44
		80.0	65.1	68.0 ± 1.4	0.002 ± 2.16	0.963	5.52
		180	78.6	80.8 ± 2.3	0.002 ± 4.54	0.976	19.4
	303	40.0	36.1	37.5 ± 0.6	0.005 ± 0.001	0.962	1.27
Pb^{2+}		80.0	65.8	68.6 ± 1.1	0.002 ± 0.001	0.971	3.96
		180	79.7	78.4 ± 1.5	0.005 ± 0.001	0.965	9.72
	313	40.0	36.9	39.4 ± 0.9	0.005 ± 0.001	0.938	2.53
		80.0	66.3	69.3 ± 1.1	0.003 ± 0.001	0.974	1.86
		180	85.1	82.2 ± 2.2	0.004 ± 9.9	0.927	0.248
	293	15.0	13.6	13.9 ± 0.5	0.012 ± 0.002	0.900	0.535
		25.0	16.5	16.6 ± 0.2	0.021 ± 0.002	0.972	0.108
		50.0	23.1	23.9 ± 0.3	0.016 ± 0.002	0.954	0.346
	303	15.0	13.9	14.1 ± 0.2	0.025 ± 0.003	0.972	0.139
Zn^{2+}		25.0	17.7	17.4 ± 0.4	0.021 ± 0.005	0.938	0.657
		50.0	25.1	25.9 ± 0.5	0.014 ± 0.002	0.934	0.615
	313	15.0	14.2	14.3 ± 0.1	0.030 ± 0.002	0.987	0.028
		25.0	18.3	18.5 ± 0.3	0.020 ± 0.002	0.942	0.263
		50.0	26.0	26.1 ± 0.1	0.020 ± 0.001	0.987	0.068
	Elovich equation						
	T (K)	C_0 (mg L^{-1})	$q_{e(exp)}$ (mg g^{-1})	α (g mg^{-1} min^{-1})	β (g mg^{-1})	R^2	SSE × 10^2
	293	40.0	35.7	13.3 ± 2.49	4.83 ± 0.654	0.843	8.68
		80.0	65.1	14.9 ± 2.72	10.5 ± 0.713	0.955	6.75
		180	78.6	29.9 ± 4.40	10.3 ± 1.16	0.886	17.7
	303	40.0	36.1	14.0 ± 2.24	4.72 ± 0.589	0.864	4.60
Pb^{2+}		80.0	65.8	18.3 ± 2.53	10.0 ± 0.666	0.957	5.88
		180	79.7	44.4 ± 2.54	7.10 ± 0.666	0.918	5.89
	313	40.0	36.9	13.7 ± 3.04	5.26 ± 0.832	0.812	7.63
		80.0	66.3	22.4 ± 3.72	9.63 ± 1.02	0.908	11.4
		180	85.1	43.6 ± 2.69	8.33 ± 0.734	0.934	5.94
	293	15.0	13.6	4.35 ± 0.391	1.93 ± 0.11	0.976	0.128
		25.0	16.5	8.92 ± 0.681	1.60 ± 0.19	0.901	0.387
		50.0	23.1	14.1 ± 1.54	2.03 ± 0.21	0.835	1.98
	303	15.0	13.9	7.81 ± 0.54	1.32 ± 0.15	0.909	1.70
Zn^{2+}		25.0	17.7	9.70 ± 0.64	1.64 ± 0.17	0.917	0.338
		50.0	25.1	15.2 ± 1.8	2.22 ± 0.49	0.806	2.73
	313	15.0	14.2	8.74 ± 0.50	1.17 ± 0.14	0.901	0.201
		25.0	18.3	10.2 ± 0.62	1.74 ± 0.17	0.928	0.322
		50.0	26.0	17.5 ± 0.90	1.82 ± 0.25	0.871	0.678

Table 3
Thermodynamic parameters of Pb^{2+} and Zn^{2+} adsorption by IDA-LG

Metal ion	E_a (kJ mol^{-1})	ΔH (kJ mol^{-1})	ΔS (J mol^{-1} K^{-1})	ΔG (kJ mol^{-1})		
				293 K	303 K	313 K
Pb^{2+}	12.0	36.1	138	–4.18	–6.15	–6.94
Zn^{2+}	33.6	1.96	30	–6.23	–6.54	–6.79

3.2.5. Thermodynamic analysis

Thermodynamics often reflect the true state of reaction from the following aspects. Gibbs free energy ΔG represents the spontaneity of chemical reaction, apparent activation energy E_a reflects the difficulty of reaction, ΔH and ΔS represent the changes of enthalpy and entropy accompanying the reaction. The calculation formula for the thermodynamic parameters of IDA-LG adsorption Pb^{2+} and Zn^{2+} was as follows:

$$\Delta G = -RT\ln K_c \tag{10}$$

In which K_c can be calculated according to Eq. (13):

$$K_c = \frac{C_{ad}}{C_e} \tag{11}$$

$$\Delta G = \Delta H - T\Delta S \tag{12}$$

$$\ln k = -\frac{E_a}{RT} + \ln A \tag{13}$$

where k is the adsorption rate constant, R is the ideal gas constant, T is the adsorption reaction temperature (K), and A is the pre-exponential factor.

According to the formula, the calculated results are shown in Table 3. The adsorption of Pb^{2+} by IDA-LG was $\Delta G < 0$, $\Delta H > 0$, $\Delta S > 0$, it indicated the reaction process was spontaneously endothermic and entropy increases. $E_a < 40$ kJ mol^{-1}, $\Delta H < 84$ kJ mol^{-1}, indicated the chemical adsorption was accompanied by physical adsorption, and the results was consistent with the kinetic study. The thermodynamic result of adsorption of Zn^{2+} by IDA-LG was consistent with those of adsorption of Pb^{2+}.

3.2.6. Competitive adsorption in binary system

To explore whether IDA-LG had preferential selectivity in adsorption of Pb^{2+} and Zn^{2+}, the comparative experiment

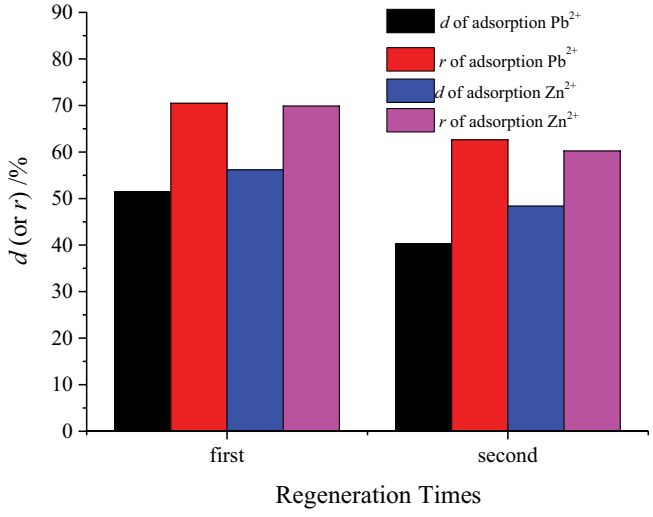

Fig. 9. The results of desorption and regeneration.

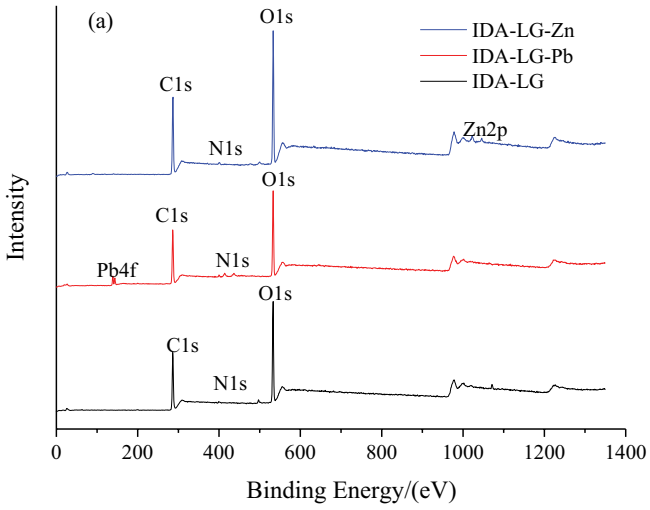

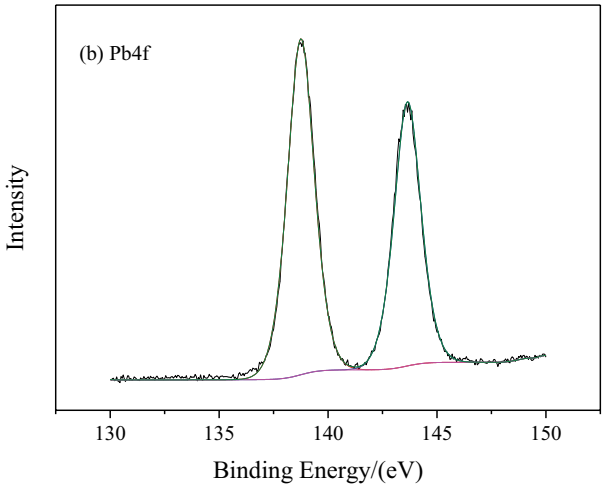

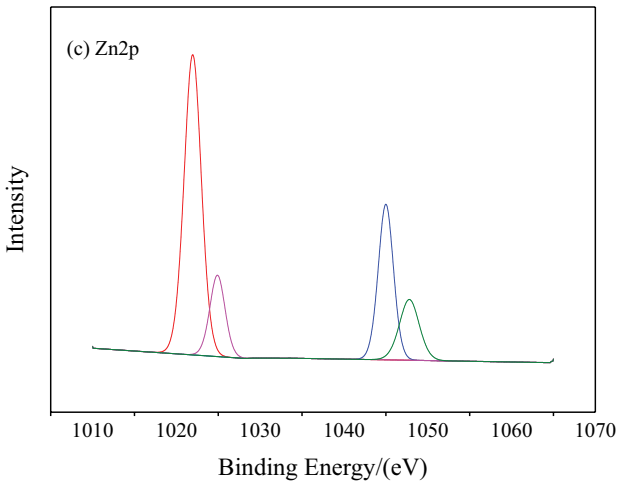

Fig. 10. (a) Full XPS spectrum of IDA-LG before and after adsorption of Pb^{2+} and Zn^{2+}, (b) Pb4f and (c) and Zn2p spectrum.

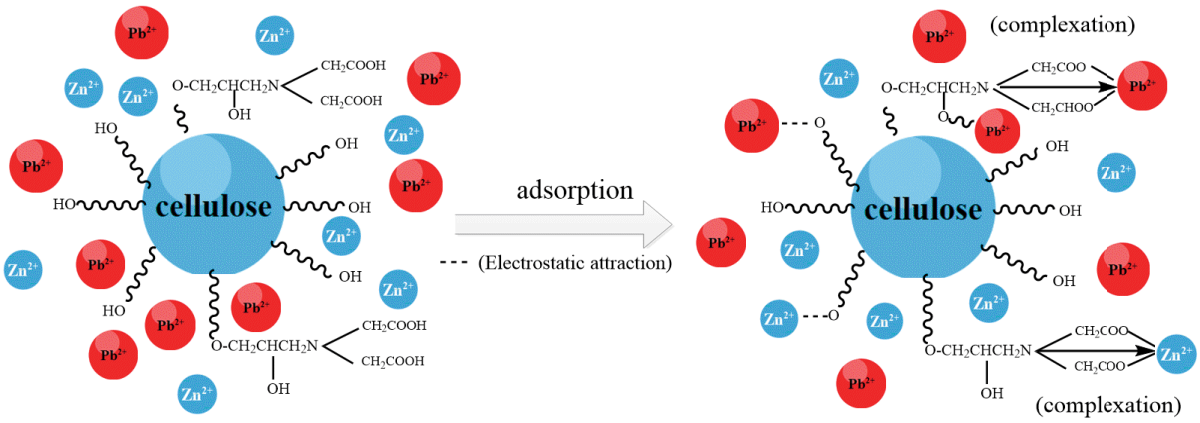

Fig. 11. The diagram of adsorption mechanism.

between single system and binary system was carried out. Adjusting the concentrations of Pb^{2+}, Zn^{2+}, and Cu^{2+} to 180, 50, 50 mg L^{-1}. The unit adsorption capacities of IDA-LG for Pb^{2+}, Zn^{2+} and Cu^{2+} were 82.5 mg g^{-1} (0.778 mmol g^{-1}), 25.2 mg g^{-1} (0.388 mmol g^{-1}) and 19.6 mg g^{-1} (0.306 mmol g^{-1}) in a single system, respectively. In the binary system, the unit adsorption capacities of IDA-LG for Pb^{2+} and Zn^{2+} were 80.5 mg g^{-1} (0.759 mmol g^{-1}) and 1.60 mg g^{-1} (0.025 mmol g^{-1}), respectively. The unit adsorption capacity of IDA-LG for Pb^{2+} and Cu^{2+} is 75.2 mg g^{-1} (0.709 mmol g^{-1}) and 7.50 mg g^{-1} (0.117 mmol g^{-1}), respectively. The unit adsorption capacity of IDA-LG for Zn^{2+} and Cu^{2+} was 4.2 mg g^{-1} (0.066 mmol g^{-1}) and 17.5 mg g^{-1} (0.270 mmol g^{-1}). These data suggested that IDA-LG had preferential selectivity for Pb^{2+} adsorption in binary system, which was similar research result from Guo et al. study [40].

3.2.7. Desorption and regeneration

The spent or exhausted adsorbent can be regenerated and reuse and this can afford the economic process [41–45]. For fully reflect the green environmental chemistry guidelines and explore whether IDA-LG can be reused. In this study, 0.1 mol L^{-1} HCl, 0.1 mol L^{-1} HNO_3, 75% ethanol, 0.1 mol L^{-1} $Ca(NO_3)_2$ and a mixture of these desorption solutions are used to desorb and regenerate the material. The results are shown in Fig. 9. It is seen from Fig. 9 that 0.1 mol L^{-1} HNO_3 + 0.1 mol L^{-1} $Ca(NO_3)_2$ had the best desorption effect on IDA-LG adsorption of Pb^{2+} and Zn^{2+}, which may be because as the acidity in the solution increases. The H^+ in the solution increases, it could exchange with Pb^{2+} and Zn^{2+} on the surface of IDA-LG, salt ions inhibited adsorption progress, thereby desorbing Pb^{2+} and Zn^{2+}. Selected 0.1 mol L^{-1} HNO_3 + 0.1 mol L^{-1} $Ca(NO_3)_2$ to desorb and regenerate the material twice. Both regeneration rates were above 60%. The results indicated that the material had a certain recycling ability.

3.3. X-ray photoelectron spectroscopy analysis and mechanism prediction

X-ray photoelectron spectroscopy (XPS) can perform the qualitative composition of material. IDA-LG and Zn or Pb loaded IDA-LG are characterized by XPS. The full spectrum of XPS and each peak diagram are shown in Fig. 10a. IDA-LG is mainly composed of C, O, N elements, which contents were 60.61%, 38.11% and 1.28%, respectively. The adsorption of Pb^{2+} by IDA-LG mainly contains C, O, N and Pb, while the adsorption of Zn^{2+} by IDA-LG mainly contains C, O, N and Zn. Fig. 10b was the peak dividing diagram of Pb4f. There are Pb3d peaks at the binding energies of 138.97 and 139.06 eV [46], which indicating that Pb^{2+} had been successfully adsorbed to IDA-LG. Fig. 10c shows the peak division of Zn2p. There was the Zn2p peak at the binding energy of 1,045.01 eV, which was the binding energy of Zn–O bond. It represented the coordination reaction between Zn and the carboxyl group on IDA-LG [47]. The interaction between IDA-LG and Pb^{2+} and Zn^{2+} was mainly consistent with complexation. Fig. 11 is a mechanism diagram between IDA-LG and Pb^{2+} or Zn^{2+}.

4. Conclusion

In this study, a new adsorption material modified by iminodiacetic acid (IDA-LG) was prepared by epoxidation and cross-linking. The adsorption capacity is enhanced after modification. The adsorption of Pb^{2+} onto IDA-LG was mainly monolayer adsorption while adsorption of Zn^{2+} was heterogeneous chemical adsorption process. Both Cu^{2+} and Pb^{2+} are accompanied by ion exchange. The binary competition system verified that the preferential selectivity of adsorption was toward Pb^{2+}. IDA-LG can be used as a novel adsorbent with bright research prospects in the research of removing heavy metals from solution.

Acknowledgements

This work was financially supported by the Henan province basis and advancing technology research project (142300410224).

References

[1] S.-L. Wang, X.-R. Xu, Y.-X. Sun, J.-L. Liu, H.-B. Li, Heavy metal pollution in coastal areas of South China: a review, Mar. Pollut. Bull., 76 (2013) 7–15.

[2] R. Shrestha, S. Ban, S. Devkota, S. Sharma, R. Joshi, A.P. Tiwari, H.Y. Kim, M.K. Joshi, Technological trends in heavy metals removal from industrial wastewater: a review, J. Environ. Chem. Eng., 9 (2021) 105688, doi: 10.1016/j.jece.2021.105688.
[3] H.Q. Qin, T.J. Hu, Y.B. Zhai, N.Q. Lu, J. Aliyeva, The improved methods of heavy metals removal by biosorbents: a review, Environ. Pollut., 258 (2020) 113777, doi: 10.1016/j.envpol.2019.113777.
[4] J. Mo, Q. Yang, N. Zhang, W. Zhang, Y. Zheng, Z. Zhang, A review on agro-industrial waste (AIW) derived adsorbents for water and wastewater treatment, J. Environ. Manage., 227 (2018) 395–405.
[5] A.A. Alqadami, Mu. Naushad, Z.A. ALOthman, M. Alsuhybani, M. Algamdi, Excellent adsorptive performance of a new nanocomposite for removal of toxic Pb(II) from aqueous environment: adsorption mechanism and modeling analysis, J. Hazard. Mater., 389 (2020) 121896, doi: 10.1016/j.jhazmat.2019.121896.
[6] Q. Du, S. Zhang, J. Song, Y. Zhao, F. Yang, Activation of porous magnetized biochar by artificial humic acid for effective removal of lead ions, J. Hazard. Mater., 389 (2020) 122115, doi: 10.1016/j.jhazmat.2020.122115.
[7] S. Liu, Z. Xie, Y. Zhu, Y. Zhu, Y. Jiang, Y. Wang, H. Gao, Adsorption characteristics of modified rice straw biochar for Zn and in-situ remediation of Zn contaminated soil, Environ. Technol. Innov., 22 (2021) 101388, doi: 10.1016/j.eti.2021.101388.
[8] F.M. Mpatani, A.A. Aryee, A.N. Kani, R.P. Han, Z.H. Li, E. Dovi, L.B. Qu, A review of treatment techniques applied for selective removal of emerging pollutant-trimethoprim from aqueous systems, J. Cleaner Prod., 308 (2021) 127359, doi: 10.1016/j.jclepro.2021.127359.
[9] G. Crini, E. Lichtfouse, Advantages and disadvantages of techniques used for wastewater treatment, Environ. Chem. Lett., 17 (2019) 145–155.
[10] E. Repo, J.K. Warchoł, A. Bhatnagar, A. Mudhoo, M. Sillanpää, Aminopolycarboxylic acid functionalized adsorbents for heavy metals removal from water, Water Res., 47 (2013) 4812–4832.
[11] W.S. Chai, J.Y. Cheun, P. Senthil Kumar, M. Mubashir, Z. Majeed, F. Banat, S.-H. Ho, P.L. Show, A review on conventional and novel materials towards heavy metal adsorption in wastewater treatment application, J. Cleaner Prod., 296 (2021) 126589, doi: 10.1016/j.jclepro.2021.126589.
[12] G. Crini, E. Lichtfouse, L.D. Wilson, N. Morin-Crini, Conventional and non-conventional adsorbents for wastewater treatment, Environ. Chem. Lett., 17 (2019) 195–213.
[13] K.S. Bharathi, S.T. Ramesh, Removal of dyes using agricultural waste as low-cost adsorbents: a review, Appl. Water Sci., 3 (2013) 773–790.
[14] X. Xu, B. Gao, B. Jin, Q. Yue, Removal of anionic pollutants from liquids by biomass materials: a review, J. Mol. Liq., 215 (2016) 565–595.
[15] J.L. Wang, X. Liu, M.M. Yang, H.Y. Han, S.S. Zhang, G.F. Ouyang, R.P. Han, Removal of tetracycline using modified wheat straw from solution in batch and column modes, J. Mol. Liq., 338 (2021) 116698, doi: 10.1016/j.molliq.2021.116698.
[16] F.M. Mpatani, A.A. Aryee, A.N. Kani, Q.H. Guo, E. Dovi, L.B. Qu, Z.H. Li, R.P. Han, Uptake of micropollutant-bisphenol A, methylene blue and neutral red onto a novel bagasse-β-cyclodextrin polymer by adsorption process, Chemosphere, 259 (2020) 127439, doi: 10.1016/j.chemosphere.2020.127439.
[17] J.Y. Li, J. Ma, Q.H. Guo, S.L. Zhang, H.Y. Han, S.S. Zhang, R.P. Han, Adsorption of hexavalent chromium using modified walnut shell from solution, Water Sci. Technol., 81 (2020) 824–833.
[18] B.L. Zhao, W. Xiao, Y. Shang, H.M. Zhu, R.P. Han, Adsorption of light green anionic dye using cationic surfactant-modified peanut husk in batch mode, Arabian J. Chem., 10 (2017) S3595–S3602.
[19] Y. Tian, M. Wu, X. Lin, P. Huang, Y. Huang, Synthesis of magnetic wheat straw for arsenic adsorption, J. Hazard. Mater., 193 (2011) 10–16.
[20] M.P. Elizalde-González, J. Mattusch, R. Wennrich, Chemically modified maize cobs waste with enhanced adsorption properties upon methyl orange and arsenic, Bioresour. Technol., 99 (2008) 5134–5139.
[21] I. Anastopoulos, I. Pashalidis, Environmental applications of *Luffa cylindrica*-based adsorbents, J. Mol. Liq., 319 (2020) 114127, doi: 10.1016/j.molliq.2020.114127.
[22] D.K. Verma, S.H. Hasan, D. Ranjan, R.M. Banik, Modified biomass of *Phanerochaete chrysosporium* immobilized on luffa sponge for biosorption of hexavalent chromium, Int. J. Environ. Sci. Technol., 11 (2014) 1927–1938.
[23] D. Pathania, A. Sharma, V. Sethi, Microwave induced graft copolymerization of binary monomers onto *Luffa cylindrica* fiber: removal of congo red, Procedia Eng., 200 (2017) 408–415.
[24] A.A. Aryee, F.M. Mpatani, Y. Du, A.N. Kani, E. Dovi, R. Han, Z. Li, L. Qu, Fe_3O_4 and iminodiacetic acid modified peanut husk as a novel adsorbent for the uptake of Cu(II) and Pb(II) in aqueous solution: Characterization, equilibrium and kinetic study, Environ. Pollut., 268 (2021) 115729, doi: 10.1016/j.envpol.2020.115729.
[25] Y. Zhang, L. Zhu, Y. Wang, Z. Lou, W. Shan, Y. Xiong, Y. Fan, Preparation of a biomass adsorbent for gallium(III) based on corn stalk modified by iminodiacetic acid, J. Taiwan Inst. Chem. Eng., 91 (2018) 291–298.
[26] Mu. Naushad, T. Ahamad, K.M. Al-Sheetan, Development of a polymeric nanocomposite as a high performance adsorbent for Pb(II) removal from water medium: equilibrium, kinetic and antimicrobial activity, J. Hazard. Mater., 407 (2021) 124816, doi: 10.1016/j.jhazmat.2020.124816.
[27] H. Wang, X. Yuan, Y. Wu, H. Huang, G. Zeng, Y. Liu, X. Wang, N. Lin, Y. Qi, Adsorption characteristics and behaviors of graphene oxide for Zn(II) removal from aqueous solution, Appl. Surf. Sci., 279 (2013) 432–440.
[28] A.A. Aryee, F.M. Mpatani, X.T. Zhang, A.N. Kani, E. Dovi, R.P. Han, Z.H. Li, L.B. Qu, Iron(III) and iminodiacetic acid functionalized magnetic peanut husk for the removal of phosphate from solution: characterization, kinetic and equilibrium studies, J. Cleaner Prod., 268 (2020) 122191, doi: 10.1016/j.jclepro.2020.122191.
[29] G. Yuvaraja, Y. Pang, D.Y. Chen, L.J. Kong, S. Mehmood, M.V. Subbaiah, D.S. Rao, C. Mouli Pavuluri, J.C. Wen, G.M. Reddy, Modification of chitosan macromolecule and its mechanism for the removal of Pb(II) ions from aqueous environment, Int. J. Biol. Macromol., 136 (2019) 177–188.
[30] S. Çete, E. Turan, E. Yildirim, T. Çaykara, Myoglobin adsorption onto poly(glycidyl methacrylate) microbeads with surface functionalized iminodiacetic acid, Mater. Sci. Eng., C, 29 (2009) 20–24.
[31] M.A. Aslam, W. Ding, S. ur Rehman, A. Hassan, Y. Bian, Q. Liu, Z. Sheng, Low cost 3D bio-carbon foams obtained from wheat straw with broadened bandwidth electromagnetic wave absorption performance, Appl. Surf. Sci., 543 (2021) 148785, doi: 10.1016/j.apsusc.2020.148785.
[32] A.E. Orduz, C. Acebal, G. Zanini, Activated carbon from peanut shells: 2,4-D desorption kinetics study for application as a green material for analytical purposes, J. Environ. Chem. Eng., 9 (2021) 104601, doi: 10.1016/j.jece.2020.104601.
[33] Y.F. Gu, M.Y. Liu, M.M. Yang, W.L. Wang, S.S. Zhang, R.P. Han, Adsorption of light green anionic dye from solution using polyethyleneimine-modified carbon nanotubes in batch mode, Desal. Water Treat., 138 (2019) 368–378.
[34] X. Jin, Z. Xiang, Q. Liu, Y. Chen, F. Lu, Polyethyleneimine-bacterial cellulose bioadsorbent for effective removal of copper and lead ions from aqueous solution, Bioresour. Technol., 244 (2017) 844–849.
[35] A. Naskar, R. Majumder, Understanding the adsorption behaviour of acid yellow 99 on *Aspergillus niger* biomass, J. Mol. Liq., 242 (2017) 892–899.
[36] M. Vesali-Naseh, M.R. Vesali Naseh, P. Ameri, Adsorption of Pb(II) ions from aqueous solutions using carbon nanotubes: a systematic review, J. Cleaner Prod., 291 (2021) 125917, doi: 10.1016/j.jclepro.2021.125917.
[37] A. Terdputtakun, O.-a. Arqueropanyo, P. Sooksamiti, S. Janhom, W. Naksata, Adsorption isotherm models and error analysis for single and binary adsorption of Cd(II) and Zn(II) using

leonardite as adsorbent, Environ. Earth Sci., 76 (2017) 777, doi: 10.1007/s12665-017-7110-y.
[38] G.K. Rajahmundry, C. Garlapati, P.S. Kumar, R.S. Alwi, D.-V.N. Vo, Statistical analysis of adsorption isotherm models and its appropriate selection, Chemosphere, 276 (2021) 130176, doi: 10.1016/j.chemosphere.2021.130176.
[39] X.T. Zhang, C.H. Ma, K. Wen, R.P. Han, Adsorption of phosphate from aqueous solution by lanthanum modified macroporous chelating resin, Korean J. Chem. Eng., 37 (2020) 766–775.
[40] S. Guo, P. Jiao, Z. Dan, N. Duan, J. Zhang, G. Chen, W. Gao, Synthesis of magnetic bioadsorbent for adsorption of Zn(II), Cd(II) and Pb(II) ions from aqueous solution, Chem. Eng. Res. Des., 126 (2017) 217–231.
[41] H.N. Bhatti, Z. Mahmood, A. Kausar, S.M. Yakout, O.H. Shair, M. Iqbal. Biocomposites of polypyrrole, polyaniline and sodium alginate with cellulosic biomass: adsorption–desorption, kinetics and thermodynamic studies for the removal of 2,4-dichlorophenol, Int. J. Biol. Macromol., 153 (2020) 146–157.
[42] S.S. Chen, Z.Y. Zang, S.S. Zhang, G.F. Ouyang, R.P. Han, Preparation of MIL-100(Fe) and multi-walled carbon nanotubes nanocomposite with high adsorption capacity towards oxytetracycline from solution, J. Environ. Chem. Eng., 9 (2021) 104780, doi: 10.1016/j.jece.2020.104780.
[43] H.J. Wang, Q. Liu, Z.Q. Wang, R.P. Han, Adsorption of CDMA from solution in batch mode using chemical activated pyrolytic char, Desal. Water Treat., 231 (2021) 367–376.
[44] N.I. Taib, N.A. Rosli, N.I. Saharrudin, N.M. Rozi, N.A.A. Kasdiehram, N.N.T. Abu Nazri, Kinetic, equilibrium, and thermodynamic studies of untreated watermelon peels for removal of copper(II) from aqueous solution, Desal. Water Treat., 227 (2021) 289–299.
[45] J. Iqbal, N.S. Shah, M. Sayed, N.K Niazi, M. Imran, J.A. Khan, Z.U.H. Khan, A.G.S. Hussien, K. Polychronopoulou, F. Howari, Nano-zerovalent manganese/biochar composite for the adsorptive and oxidative removal of Congo-red dye from aqueous solutions, J. Hazard. Mater., 403 (2021) 123854, doi: 10.1016/j.jhazmat.2020.123854.
[46] Y. Chen, Z. Yang, Q. Zhang, D. Fu, P. Chen, R. Li, H. Liu, Y. Wang, Y. Liu, W. Lv, G. Liu, Effect of tartaric acid on the adsorption of Pb(II) via humin: Kinetics and mechanism, J. Taiwan Inst. Chem. Eng., 107 (2020) 79–88.
[47] X. He, T. Zhang, Q. Xue, Y. Zhou, H. Wang, N.S. Bolan, R. Jiang, D.C.W. Tsang, Enhanced adsorption of Cu(II) and Zn(II) from aqueous solution by polyethyleneimine modified straw hydrochar, Sci. Total Environ., 778 (2021) 146116, doi: 10.1016/j.scitotenv.2021.146116.